*J Appl Physiol* 138: 182–194, 2025.
*First published November 29, 2024; doi:10.1152/japplphysiol.00379.2024*

american physiological society

JOURNAL OF APPLIED PHYSIOLOGY

RESEARCH ARTICLE

# Combined exercise hinders the progression of pulmonary and right heart harmful remodeling in monocrotaline-induced pulmonary arterial hypertension

**Luciano Bernardes Leite,[1] Leôncio Lopes Soares,[1] Alexandre Martins Oliveira Portes,[2] Bruna Aparecida Fonseca da Silva,[1] Taís Rodrigues Dias,[1] Thayana Inácia Soares,[1] Mirian Quintão Assis,[3] Luiz Otávio Guimarães-Ervilha,[3] Miguel Araújo Carneiro-Júnior,[1] Pedro Forte,[4,5,6] Mariana Machado-Neves,[3] Emily Correna Carlo Reis,[7] and Antônio José Natali[1]**

*[1]Department of Physical Education, Laboratory of Exercise Biology, Federal University of Viçosa, Viçosa, Brazil; [2]Department of Biological Sciences, Federal University of Ouro Preto, Ouro Preto, Brazil; [3]Department of General Biology, Laboratory of Structural Biology, Federal University of Viçosa, Viçosa, Brazil; [4]Research Center for Physical Activity and Wellbeing (Livewell), Polytechnic Institute of Bragança, Bragança, Portugal; [5]CI-ISCE, Higher Instituto of Educational Sciences of the Douro, Penafiel, Portugal; [6]Department of Sports, Higher Institute of Educational Sciences of the Douro, Penafiel, Portugal; and [7]Veterinary Department, Federal University of Viçosa, Viçosa, Brazil*

## Abstract

The aim of this study was to test whether combined physical exercise training of moderate intensity executed during the development of monocrotaline (MCT)-induced pulmonary arterial hypertension (PAH) hinders the progression of pulmonary and right heart harmful functional and structural remodeling in rats. Wistar rats were injected with MCT (60 mg/kg) and after 24 h were exposed to a combined exercise training program: aerobic exercise (treadmill running—60 min/day; 60% of maximum running speed); and resistance exercise (vertical ladder climbing—15 climbs; 60% of maximum carrying load), on alternate days, 5 days/wk, for ∼3 wk. After euthanasia, the lung and right ventricle (RV) were excised and processed for histological, single myocyte, and biochemical analyses. Combined exercise increased the tolerance to physical effort (time until fatigue and relative maximum load) and prevented increases in pulmonary artery resistance (acceleration time (TA)/ejection time (TE)] and reductions in RV function [tricuspid annular plane systolic excursion (TAPSE)]. Moreover, in myocytes isolated from the RV, combined exercise preserved contraction amplitude, as well as contraction and relaxation velocities, and inhibited reductions in the amplitude and maximum speeds to peak and to decay of the intracellular $Ca^{2+}$ transient. Furthermore, combined exercise avoided RV (RV weight, cardiomyocyte, extracellular matrix, collagen, inflammatory infiltrate, and extracellular matrix) and lung (pulmonary alveoli and alveolar septum) harmful structural remodeling. In addition, combined exercise restricted RV [nitric oxide (NO) and carbonyl protein (CP)] and lung [catalase (CAT), glutathione S-transferase (GST), and NO] oxidative stress. In conclusion, the applied combined exercise regime hinders the progression of pulmonary and right heart functional and structural harmful remodeling in rats with MCT-induced PAH.

**NEW & NOTEWORTHY** This study reveals that combined exercise improves tolerance to physical effort, prevents increases in pulmonary artery resistance, and conserves the right heart function during the progression of pulmonary arterial hypertension. Our analyses show that combined exercise hinders harmful right ventricular and lung structural remodeling and oxidative stress, which reflects in the maintenance of right ventricular myocytes' contractile function by preserving the intracellular calcium cycling. An attenuated progression of the disease impacts positively on its prognosis.

*combined exercise training; isolated myocytes; oxidative stress; pulmonary arterial hypertension; remodeling*

## INTRODUCTION

Monocrotaline (MCT) has been adopted as an effective model for the induction of pulmonary arterial hypertension (PAH) and right heart failure in rats. When metabolized by the liver, MCT produces dehydromonocrotaline, a toxic metabolite that causes progressive hypertension due to pulmonary mononuclear vasculitis and hence structural remodeling of pulmonary vessels including the pulmonary artery (1, 2). As a result of lung dysfunctions, the right ventricle (RV) is overloaded, which generates a pathologic compensatory hypertrophy (3) followed by failure and death (4).

Oxidative stress has been considered a key factor in both pulmonary (5–8) and right heart reshaping (9–12) in the rat model of MCT-induced PAH. Disruptions in fundamental elements regulating the redox homeostasis in the lung and

Correspondence: L. B. Leite (luciano.leite@ufv.br).
Submitted 22 May 2024 / Revised 30 September 2024 / Accepted 20 November 2024

in the RV have been reported. For instance, in the lung MCT is known to increase oxygen reactive species (ROS) and to elevate the production of oxidants [e.g., superoxide, hydrogen peroxide, and nitric oxide (NO)] and/or decrease the antioxidant defenses [e.g., catalase (CAT), superoxide dismutase (SOD), and glutathione S-transferase (GST)] (7, 13). Such imbalance in association with other stimuli (e.g., increased transmural pressure, shear stress, hypoxia, mediators like angiotensin II, endothelin 1, growth factors, and inflammatory cytokines) leads to endothelial dysfunction and hence vasoconstriction (5). Increases in lung mass, thickenings of alveolar septum, and reductions in alveolar area, as well as the presence of collapsed and hemorrhagic alveoli, are observed, which results in a lower number of alveoli and worsened functionality (13–17). In the RV of rats with MCT-induced PAH, the redox homeostasis is also disturbed (7, 12, 17–20). Such disturbance causes functional and structural adverse remodeling as it triggers extracellular matrix remodeling and increases fibrosis (21). Furthermore, excessive ROS diminishes the RV myocyte contractility since it damages the $Ca^{2+}$ cycling regulatory proteins at the cellular level (22, 23). As a result, the functionality of the right heart is impaired (17).

Regarding nonpharmacological therapies, combined physical exercise has been recommended for hypertensive individuals (24, 25) and has demonstrated improvements in muscle power, tolerance to physical effort, and the quality of life of individuals with PAH (26–28). Studies on the MCT-induced PAH model in rats have demonstrated that low- to moderate-intensity aerobic or resistance exercise trainings, when performed individually, increase tolerance to physical effort and survival, prevent pathological remodeling of the RV and lungs, and promote benefits to the right heart functionality as well as to contractile function and intracellular $Ca^{2+}$ transient in single ventricular myocytes (17, 29, 30). Concerning oxidative stress, protective effects of aerobic (11, 13) and resistance exercise of low- to moderate-intensity (17) training executed separately have been reported in the lung, skeletal muscle, and RV in this experimental model of PAH. These effects are accompanied by the preservation of the organ functionality. Regardless of such benefits, the impact of combined physical training (i.e., aerobic plus resistance) of moderate intensity in the functional and structural remodeling of the pulmonary and right heart remains poorly understood.

## METHODS

### Study Design

Male Wistar rats at 6 wk of age were randomly distributed into three experimental groups: sedentary control (SC), sedentary hypertensive (SH), and exercise hypertensive (EH), each consisting of seven animals. All animals were kept in a temperature-controlled room (~22°C) and relative humidity of ~60%, under a 12/12-h light/dark cycle. They had free access to water and standard rodent chow. All experimental procedures were conducted following the Ethical Principles in Animal Experimentation. The research project was approved by the Ethics Committee on the Use of Animals of the Federal University of Viçosa (CEUA-UFV) under Protocol No. 02/2021.

### Induction of Pulmonary Arterial Hypertension

Animals in groups SH and EH received a single intraperitoneal injection (60 mg/kg body weight) of MCT (Sigma-Aldrich, St Louis, MO) dissolved in saline solution (140 mM NaCl; pH 7.4) (31). Animals in the SC group received the same volume of the saline solution.

### Combined Physical Training Protocol

The combined moderate-intensity physical training regimen consisted of sessions on an electric treadmill (for aerobic training) and a ladder adapted for rats (for resistance training) conducted 5 days a week (Monday to Friday) over a period of ~3 wk. Each type of exercise was performed on alternate days. The intensities of each type of training were determined based on pre-evaluation of the rat's maximum running speed on the treadmill and maximum load carried on the vertical ladder.

### Aerobic Training and Maximum Running Velocity Test

The rats underwent a 2-wk familiarization period with the electric treadmill (AVS Projetos, São Paulo, Brazil). During the first week, they engaged in short periods of light exercise (5 min, no incline, 5 m/min) for 3 days, alternating with resistance training. In the second week, the duration of exercise was increased to 10 min per day, still without incline and at a speed of 5 m/min, for 3 days (alternating with resistance training). Forty-eight hours after the adaptation period, the physical effort tolerance test was conducted using a progressive treadmill exercise protocol, as previously described (32).

The initial running velocity was set at 5 m/min, with increments of 3 m/min every 3 min, and no incline, until fatigue. Fatigue was defined as the point at which the animals could no longer maintain the running pace corresponding to the treadmill speed. The total time and maximum running velocity achieved by each rat were recorded. This test was conducted three times: 2 days after familiarization with the equipment, on the 12th and 19th days following MCT injection. The total time to fatigue (TTF) was used as an index of aerobic physical effort tolerance.

Subsequently, animals in the EH groups underwent a moderate-intensity running training protocol on a treadmill (32). The training began 24 h after MCT administration, utilizing an electric treadmill (AVS Projetos, São Paulo, Brazil). Training sessions were conducted 2 to 3 days per week, alternating with resistance training, with each session lasting 60 min. Each session comprised a warm-up period [5 min; speed set at 20% of maximum running velocity (MRV)], a training period (50 min; speed set at 60% of MRV), and a cool-down period (5 min; speed set at 20% of MRV). During the first week, the initial speed was set at 5 m/min, with increments of 3 m/min every 3 min until reaching 60% of MRV. At the end of the second week of training, running intensities were readjusted based on the MRV obtained in the exercise tolerance test.

### Resistance Training and Maximal Load Test

Regarding resistance training, the rats underwent a 2-wk familiarization period with the exercise model, which involved climbing a vertical ladder (height: 1.1 m; width: 0.18 m; spacing

between steps: 2 cm; inclination: 80°) while carrying a load proportionate to their body weight, attached to an apparatus fixed to their tail. During the first week, the animals were encouraged to perform 8–12 climbs (i.e., repetitions) and to remain at the top of the ladder for 120 s within a polypropylene box. In the second week, the animals performed three climbs while carrying an adapted load container (~15 g), without additional weight, fixed to the proximal part of their tail with adhesive tape.

For the test, during the initial climb, the rat ascended the ladder carrying 75% of its body weight. After successfully completing the climb and following a rest interval of 120 s, an additional weight of 30 g was added for the subsequent climb. This procedure was successively repeated until the rat was unable to climb to the top of the ladder. The maximum weight with which the rat was able to climb was considered the maximum load carried. The maximum load test was conducted at three time points: 4 days after adaptation to the exercise model, on the 14th day, and on the 21st day after MCT administration. The maximum carrying load (MCL) was utilized as another index of tolerance to physical effort tolerance.

Resistance training commenced 48 h after MCT injection, employing a vertical ladder adapted for rats (33). Based on the individual maximum load test results, the animals underwent resistance training sessions 2 to 3 days per week, alternating with aerobic training, for ~4 wk. Each resistance training session comprised 15 climbs, with a 1-min rest period between climbs (34). The training sessions were conducted at an intensity corresponding to 60% of the maximum load attained in the maximum tests, thus classified as moderate.

### Echocardiography

The echocardiographic examination was conducted on the 22nd day following the MCT injection. Animals were immobilized under anesthesia (3% Isoflurane in 100% oxygen for induction and 1.5% for maintenance, with a constant flow of 1 L/min Isoflurane (BioChimico, Itatiaia RJ, Brazil), and images were acquired while the animals remained in lateral decubitus position. Two-dimensional studies with a rapid sampling rate of 120 fps (frames per second) in M-mode were performed using the MyLabTM30 ultrasound system (Esaote, Genoa, Italy) and 10 MHz nominal frequency transducers. Two-dimensional transthoracic echocardiography and M-Mode were obtained at a scanning speed of 200 mm/s adjusted according to the heart rate. Right ventricular acceleration time (TA) and ejection time (TE) values were acquired using pulsed Doppler.

The right ventricular systolic function was assessed based on a systolic excursion in the annular plane of the tricuspid valve (TAPSE—tricuspid annular plane systolic excursion). For this purpose, M-mode imaging was utilized with the cursor positioned on the lateral aspect of the annular plane of the tricuspid valve. Shortening from the base to the apex during systole was measured, identifying the lateral annulus of the tricuspid valve, the end-diastolic, and end-systolic distances. Images were captured in accordance with the recommendations of the American Society of Echocardiography and subsequently stored for subsequent analysis (35). The following RV parameters were evaluated: systolic function using TAPSE, TA, and TE, and subsequently, the TA/TE ratio was calculated.

### Sample Collection

Rats from SC, SH, and EH groups were euthanized by decapitation on the 23rd day after MCT injection. Twenty-three days represent the average end point time of non-treated male Wistar rats injected with 60 mg/kg body weight in our laboratory (30, 36). After euthanasia, the heart, RV, and lung were dissected, weighed, and processed for the analyses of interest as described later.

### Isolation of Right Ventricular Myocytes

RV myocytes were enzymatically isolated following a previously described protocol (31). After euthanasia, the heart was promptly dissected, dried, and weighed. Subsequently, the heart was connected to a Langendorff retrograde perfusion system via the aorta and perfused with Tyrode's solution containing the following components in millimoles (mM): 130 NaCl, 1.43 $MgCl_2$, 5.4 KCl, 0.75 CaCl2, 5.0 HEPES, 10.0 glucose, 20.0 taurine, and 10.0 creatine, adjusted to pH 7.4, for ~5 min. Tyrode's solution was then replaced with Tyrode's solution containing EGTA (0.1 mM) for an additional 5 min. Following this, the heart was perfused with Tyrode's solution containing 1 mg/mL type II collagenase (Worthington) and 0.1 mg/mL protease (Sigma-Aldrich) for ~12 min. The digested heart ventricles were then removed, dried, and weighed. The entire RV was also separated, weighed, and cut into small fragments. These fragments were placed in a conical flask containing the enzyme solution (collagenase and protease). Cells were mechanically separated by shaking the flask for 5 min. Subsequently, the dispersed cells were separated from the undispersed tissue by filtration. After centrifugation, the resulting cells were suspended in Tyrode's solution. The undispersed tissue was subjected to the mechanical dispersion process once again. The solutions used in the isolation procedure were oxygenated (100% $O_2$—White Martins, Brazil) and maintained at 37°C. Isolated cells were stored at 5°C until use, and they were used within 2 to 3 h after isolation.

### Measurement of Cell Contractility

Cardiomyocyte contractions were measured using the length change technique, employing the edge detection system (Ionwizard, Ionoptix) mounted on an inverted microscope (Nikon Eclipse—TS100, Japan) equipped with an oil immersion objective lens (S Fluor, ×40, Nikon), as previously described (37). Briefly, isolated myocytes were placed in the experimental chamber mounted on an inverted microscope and immersed in perfusion buffer solution (HEPES buffer solution; see Item 4.11.2) at 37°C. Myocytes were externally stimulated at a frequency of 5 Hz (10 V, 5 ms duration) using an electrical stimulator (Myopacer, Field Stimulator, Ionoptix). The image of the myocyte under evaluation was captured by a camera (Myocam, Ionoptix) attached to the inverted microscope, using image detection software (Ionwizard, Ionoptix—frequency of 240 Hz). Myocyte contraction and relaxation movements were recorded by the edge detection system (Ionwizard, Ionoptix) and stored for

later analysis of mechanical properties. Only myocytes in good condition, with well-defined borders (right and left) and sarcomeric striations, relaxed at rest and without involuntary contractions, were used in the experiments. The variables analyzed included contraction amplitude, contraction velocity, and relaxation velocity.

### Measurement of the Intracellular $Ca^{2+}$ Transient

The intracellular $Ca^{2+}$ transient measurements in myocytes isolated from the RV were performed, as previously described (38). Briefly, measurements were performed using an inverted microscope (Nikon Eclipse—TS100) equipped with an oil immersion objective lens (S Fluor, ×40, Nikon). Isolated myocytes were incubated with the fluorescent $Ca^{2+}$ indicator, Fura-2 acetoxymethyl ester (Fura-2AM, Thermo Fisher, Waltham), which is permeable to the plasma membrane. The indicator was prepared in a stock solution of dimethyl sulfoxide (DMSO), where 50 μg of Fura-2 AM was dissolved in 50 μL of DMSO. Then, 10 μL of this solution was added to 4 mL of cell medium contained in a falcon tube wrapped in thin aluminum foil. The solution was stirred on a flat surface for 10 min at a speed of ∼120 revolutions per minute. Subsequently, the tube was centrifuged at 3,000 rpm, the supernatant was removed, and the myocytes were resuspended in 4 mL of Tyrode's solution containing 750 mM CaCl2 (solution A).

The myocytes were then placed in a refrigerator at 5°C for 30 min. This entire procedure was carried out without exposing the solution and cells to light. After 30 min of rest, the intracellular $Ca^{2+}$ transient was measured using a dual excitation system that detects fluorescence excited by UV light with wavelengths of 340 and 380 nm (Ionoptix—USA). Myocytes incubated with Fura-2 were placed in an experimental chamber mounted on an inverted microscope and bathed in a perfusion buffer solution (HEPES buffer solution) at room temperature. The myocyte under evaluation was positioned within an adjustable window, with apparent edges, and stimulated externally at a frequency of 5 Hz (40 V, duration of 5 ms) using an electrical stimulator (Myopacer, Field Stimulator, Ionoptix). Fluorescence emission was detected between 340 and 380 nm by a photomultiplier tube. The recorded fluorescence is the ratio between the 340 and 380 nm excitations. Only myocytes were used that were in good condition, with well-defined borders (right and left) and sarcomeric striations, relaxed at rest and without showing involuntary contractions. Records were made up to 4 h after myocyte isolation. The variables analyzed were amplitude and velocities to peak and to decay of the intracellular $Ca^{2+}$ transient.

### Histological Analyzes

Histological and morphometric analyses were conducted following previously established protocols (39). Briefly, tissue fragments from the RV and right lung were collected, fixed in 10% formalin, dehydrated in ethanol, clarified in xylene, and embedded in paraffin. The blocks were then transversely sectioned into 5 μm thick histological sections and stained with hematoxylin-eosin (H&E) before being mounted on histology slides. To ensure thorough examination without duplication, sections were evaluated in semiseries, with one section examined for every 10 sections.

The slides were examined, and images were captured using an optical microscope (Olympus BX-50, Tokyo, Japan) equipped with a digital camera (Olympus Q Color-3, Tokyo, Japan). In the RV, the following parameters were assessed: percentage of cardiomyocytes (cytoplasm and nucleus), inflammatory infiltrate, and total collagen. In the lung, the percentage of alveolar septa and pulmonary alveoli were evaluated. ImageJ Software (National Institute of Health) was used for both analyses.

### Oxidative Stress Biomarkers

#### *Tissue preparation.*

Frozen lung and RV tissue samples (100 mg) were homogenized (using the Tissue Master 125 homogenizer, OMNI) in 1 mL of phosphate buffer (pH 7.4) and centrifuged for 10 min at 10,000 *g* (12,000 rpm), under refrigeration at 4°C. The resulting supernatants were collected for analysis of enzymatic activity of superoxide dismutase (SOD), catalase (CAT), glutathione S-transferase (GST), malondialdehyde content (MDA), nitric oxide (NO), and total protein (TP) assays. The resulting pellets were used for the analysis of carbonyl protein (CP) content. These analyses were performed in an ELISA microplate reader (Multiskan GO, Thermo Scientific) or a spectrophotometer (UV-Mini 1240, Shimadzu).

#### *Catalase activity.*

The catalase activity was determined by adapting the Hadwan method (40), using hydrogen peroxide ($H_2O_2$) as a substrate. For this, 100 μL of hydrogen peroxide (20 mmol/L) was pipetted into 5 μL samples. After 3 min, 150 μL of ammonium molybdate (32.4 mmol/L) was added to stop the reaction. Blank samples were prepared by replacing hydrogen peroxide with sodium potassium phosphate buffer (50 mmol/L, pH 7.0). The reading was taken at 374 nm on the spectrophotometer. A standard curve was prepared with serial dilution of $H_2O_2$ to calculate the CAT value. Test values were corrected by subtracting control test values to eliminate interference from other serum compounds that may react with ammonium molybdate. CAT activity was expressed as CAT KU/mg protein.

#### *Superoxide dismutase activity.*

The superoxide dismutase activity was determined according to the method described by Dieterich et al. (41). For this, 99 μL of potassium phosphate buffer (5 mmol/L, pH 8.0) were pipetted together with 30 μL of the sample and 15 μL of pyrogallol (100 μmol/L). The reaction mixture was then measured by absorbance at 570 nm. SOD activity was calculated as units per milligram of protein, with one SOD unit defined as the amount that inhibited the autoxidation rate of pyrogallol by 50%. Duplicates of blanks and standards for SOD activity were prepared without and with pyrogallol, respectively.

#### *Glutathione S-transferase activity.*

The glutathione S-transferase activity was measured using the method of Habig et al. (42). For this, 10 μL of 2,4-dinitrochlorobenzene conjugated with glutathione (CDNB) at a concentration of 1 mmol/L was added to 970 μL of buffer a 50 mmol/L, pH 7.0, together with 10 μL of reduced glutathione at 1 mmol/L and a 10 μL aliquot of the sample to be tested. After the addition of CDNB, the change in absorbance

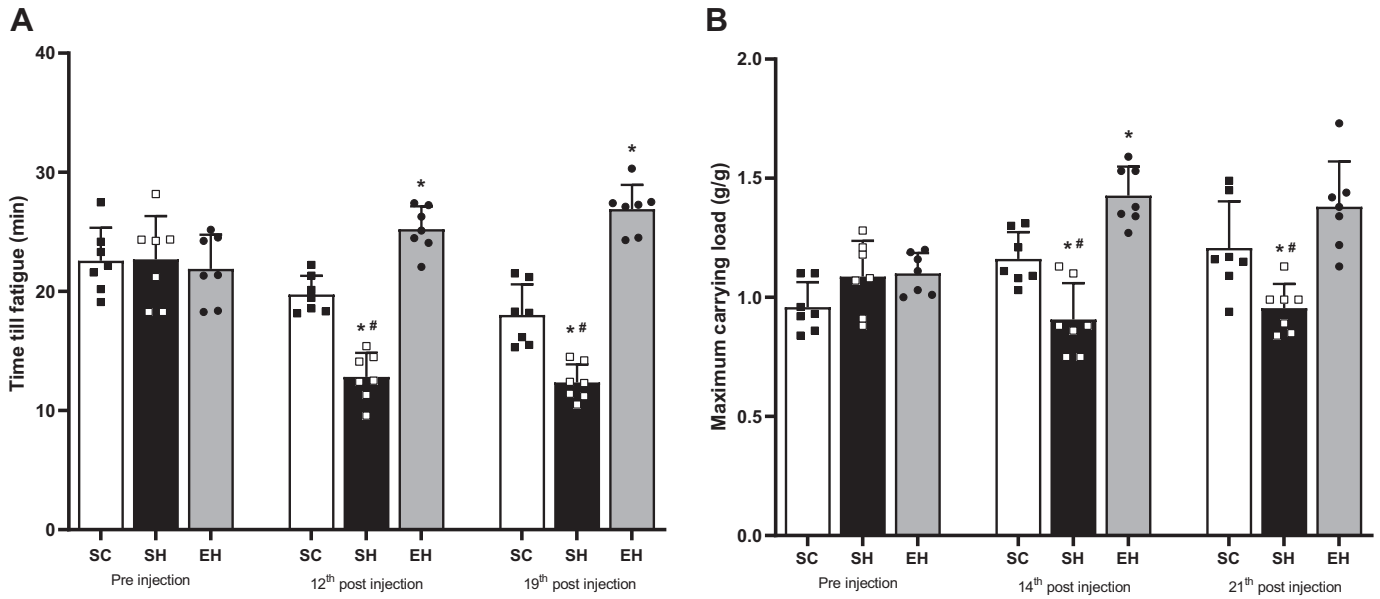


**Figure 1.** Effects of combined physical training on physical effort tolerance. *A*: total time to fatigue (TTF). *B*: maximum carrying load. Tests performed before (*day 0*), 12, 14, 19, and 21 days after the application of monocrotaline. Data are means ± SD of seven rats in each group. EH, hypertensive exercise; SC, sedentary control; SH, hypertensive sedentary. *$P < 0.05$ vs. SC; #$P < 0.05$ vs. SH. One-way ANOVA followed by Tukey's post hoc test.

was monitored at 340 nm for 60 s. The molar extinction coefficient used for CDNB was $\epsilon 340 = 9.6$ mmol/L/cm. One unit of GST activity was defined as the amount of enzyme that catalyzed the formation of one micromol of product per minute per milliliter. GST activity was expressed as micromol/min/g.

### *Malondialdehyde determination.*

Lipid peroxidation was measured according to Buege et al. (43), through the quantification of MDA, which is a product of lipid peroxidation. For this, 0.2 mL of tissue supernatant was homogenized in 0.4 mL of a solution containing 15% trichloroacetic acid, 0.375% thiobarbituric acid, and 0.6% hydrochloric acid. The reactions were left for 40 min in a water bath at 90°C. After cooling on ice, 0.6 mL of butyl alcohol was added. The solution was vortexed for 2 min and centrifuged for 10 min at 9,000 *g*. The supernatant was used to measure MDA using absorbance at 540 nm on a microplate scanning spectrophotometer (Multiskan GO). A standard curve of known concentrations of 1,1,3,3-tetramethoxypropane was used to determine the concentration of MDA. The results were expressed as micromol/L per mg of protein.

### *Nitric oxide production.*

Nitric oxide production was quantified using the standard Griess reaction, following the method described by Tsikas (44). In brief, 50 μL of samples were incubated with an equal volume of Griess reagent, composed of 1% sulfanilamide, 0.1% *N*-(1-naphthyl) ethylenediamine, and 2.5% phosphoric acid, at room temperature for 10 min. Absorbance was then measured at 570 nm using a microplate reader. Micromolar NO concentrations (μmol/L) were determined from a sodium nitrite standard curve within the concentration range of 0–100 μmol/L.

### *Protein carbonyl determination.*

The determination of protein carbonyl (PC) content was conducted using the 2,4-dinitrophenylhydrazine (DNPH) (45). In summary, pellets obtained from the extraction homogenates were mixed with 0.5 mL of 10 mmol/L DNPH solution diluted in 7% hydrochloric acid. The resulting solution was vortexed and incubated at room temperature in the dark with periodic stirring for 30 min. Subsequently, 0.5 mL of ice-cold 10% trichloroacetic acid was added to each tube, followed by centrifugation at 5,000 *g* for 10 min at 4°C. After

**Table 1.** *Body weight, organ weight, and their ratios*

| | SC | SH | EH |
|---|---|---|---|
| Initial BW, g | 197.4 ± 12.86 | 192.0 ± 8.64 | 204.4 ± 11.72 |
| Final BW, g | 307.1 ± 13.13 | 260.3 ± 23.91* | 277.6 ± 25.68* |
| Heart weight, g | 1.18 ± 0.10 | 1.44 ± 0.12*# | 1.18 ± 0.07 |
| RV weight, g | 0.23 ± 0.03 | 0.41 ± 0.07*# | 0.28 ± 0.02 |
| RV/LV, g | 0,42 ± 0,05 | 0,85 ± 0,23*# | 0,50 ± 0,06 |
| Lung weight, g | 1.86 ± 0.53 | 4.36 ± 0.60*# | 2.43 ± 0.04 |
| Heart weight/tibia length, mg/mm | 0.35 ± 0.01 | 0.47 ± 0.07*# | 0.35 ± 0.02 |
| RV weight/tibia length, mg/mm | 0.06 ± 0.01 | 0.12 ± 0.03*# | 0.08 ± 0.01 |
| Lung weight/tibia length, mg/mm | 53.52 ± 15.18 | 129.5 ± 14.80*# | 72.49 ± 5.62* |

Data are means ± SD of six or seven rats in each group; BW: body weight; EH: exercise hypertension; SC: sedentary control; SH: sedentary hypertension; RV: right ventricle. *$P < 0.05$ vs. SC. #$P < 0.05$ vs. EH. One-way ANOVA followed by Tukey's post hoc test.

centrifugation, the supernatant was discarded, and the precipitate was washed three times with 1 mL of ethyl acetate and ethanol (1:1 vol/vol). Finally, 1 mL of 6% sodium dodecyl sulfate was added, and the tubes were vortexed to dissolve the sediment. The supernatant was then measured for absorbance at 370 nm. The results were expressed in nanomol/mg of protein, based on the molar extinction coefficient of $\varepsilon 370 = 22$ mmol/L/cm.

### *Total protein.*

The determination of total protein was carried out following the method outlined by Lowry et al. in 1951 (46), utilizing bovine serum albumin as the standard. The total protein concentrations obtained were then used to standardize the results for CAT, SOD, MDA, and PC.

### Statistics

The data were subjected to the Shapiro–Wilk test to verify its distribution. For parametric data, one-way analysis of variance (one-way ANOVA) was used to evaluate between groups, followed by Tukey's post hoc test for multiple comparisons, when necessary. For nonparametric data, Kruskal–Wallis was used, followed by Dunn's post hoc for multiple comparisons, when necessary. Quantitative data are presented as means ± SE, while qualitative data are presented as percentages. An alpha error probability of up to 5% was

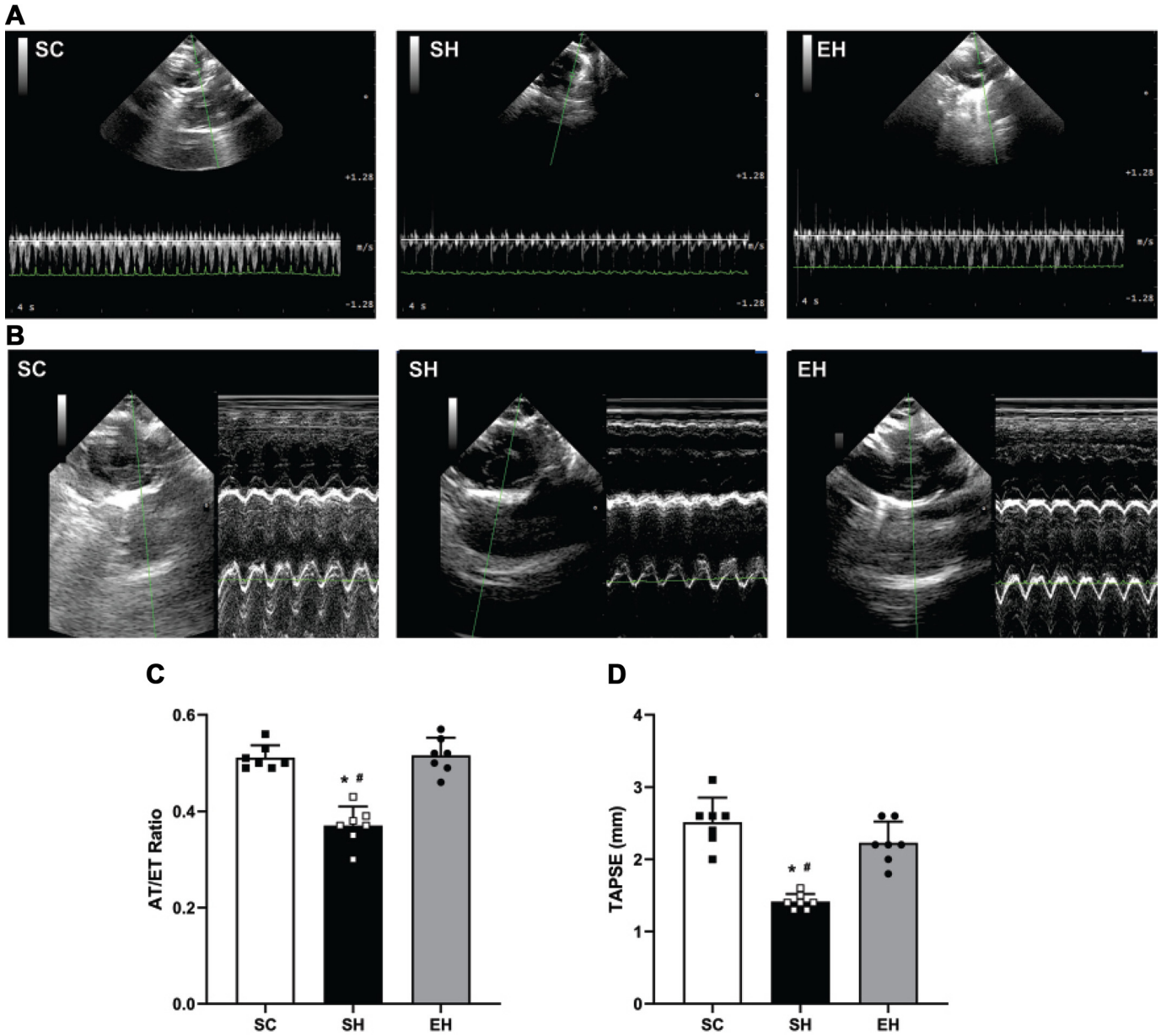


**Figure 2.** Effects of combined physical training on pulmonary artery resistance and right ventricular systolic function assessed on *day 22* after the first monocrotaline injection. *A*: representative images of pulmonary artery flow. *B*: representative image of tricuspid annular plane systolic excursion (TAPSE). *C*: acceleration time/ejection time (AT/ET) relationship. *D*: average TAPSE values. Data are means ± SD of seven mice in each group. EH, hypertensive exercise; SC, sedentary control; SH, hypertensive sedentary. One-way ANOVA followed by Tukey's post hoc test. *$P < 0.05$ vs. SC; #$P < 0.05$ vs. EH.

considered. The statistical tests and the numbers of animals and cells used in each parameter evaluated are detailed in the respective tables and figures. All analyses were performed using GraphPad Prism Software version 8.0.2.

## RESULTS

### Physical Effort Tolerance

Before MCT injection there was no difference between groups for TTF (Fig. 1*A*). However, on the 12th and 19th days after MCT injection, rats in the SH group showed lower TTF ($P < 0.05$) compared with those in the SC and EH groups. In addition, at these same time points, rats in the EH group exhibited higher TTF ($P < 0.05$) compared with those in the SC group (Fig. 1*A*). Moreover, there was no difference between groups for MCL before the MCT dose (Fig. 1*B*). However, on the 14th and 21st days after MCT needle, rats in the SH group displayed lower MCL ($P < 0.05$) than those in the SC and EH groups. Furthermore, on the 14th day, rats in the EH group had higher MCL ($P < 0.05$) compared with those in the SC group.

### Body and Organ Weights

The initial body weight was not different between groups (Table 1). However, 23 days after the injection of MCT the final weight of rats in the SH and EH groups was lower ($P < 0.05$) compared with those in the SC group. Furthermore, rats in the SH group had greater heart weight, RV weight, right lung weight, and their respective ratios ($P < 0.05$), when compared with those in the SC and EH groups, while rats in the EH group presented higher lung weight/tibia length ratio ($P < 0.05$) than those in the SC group.

### Pulmonary Artery Resistance and Right Ventricular Function

The pulmonary artery resistance was estimated by the TA/TE ratio and right ventricular systolic function was evaluated by the TAPSE (Fig. 2). Fig. 2, *A* and *B* display representative echocardiographic images of pulmonary artery flow obtained by using pulsed wave Doppler and TAPSE, respectively. On the 22nd day after the MCT injection, rats in the SH group exhibited a lower ($P < 0.05$) TA/TE ratio (Fig. 2*C*) and TAPSE (Fig. 2*D*) compared with those in the SC and EH groups.

### Myocyte Contractile Function and the Intracellular $Ca^{2+}$ Transient

Right ventricular myocytes isolated from rats in the SH group had lower ($P < 0.05$) amplitudes of contraction (Fig. 3*A*), and of the intracellular $Ca^{2+}$ transient (Fig. 3*D*)

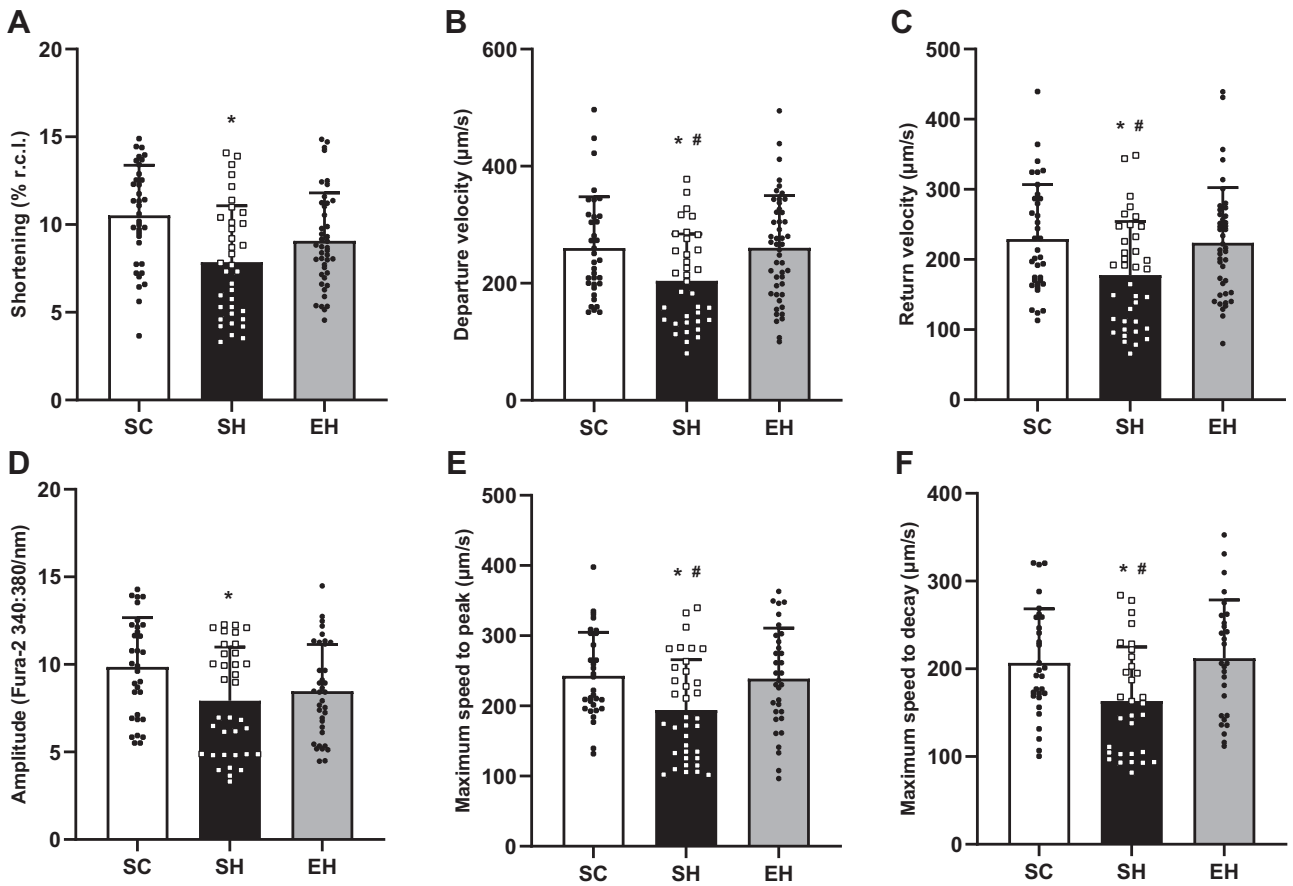


**Figure 3.** Effects of combined physical training on contractility and intracellular $Ca^{2+}$ transient in single left ventricular myocytes. *A*: amplitude of contraction. *B*: departure velocity of contraction. *C*: return velocity of contraction. *D*: amplitude of the intracellular $Ca^{2+}$ transient. *E*: maximum speed to peak of the intracellular $Ca^{2+}$ transient. *F*: maximum speed to decay of the intracellular $Ca^{2+}$ transient. Data are means ± SD of five cells per animal (six and seven animals per group). Kruskal–Wallis, test followed by Dunn's test. EH, hypertensive exercise; SC, sedentary control; SH, hypertensive sedentary. *$P < 0.05$ vs. SC; #$P < 0.05$ vs. EH.


*J Appl Physiol* • doi:10.1152/japplphysiol.00379.2024 • www.jappl.org

than those from rats in the SC group. The departure (Fig. 3*B*) and return (Fig. 3*C*) speeds of contraction as well as the maximum speeds to peak (Fig. 3*E*) and to decay (Fig. 3*F*) of the intracellular $Ca^{2+}$ transient in myocytes from rats in the SC and EH groups were higher ($P < 0.05$) compared with those from rats in the SH group.

### Right Ventricular Remodeling and Oxidative Stress

The representative photomicrographs of rats from the SC and EH showed normal and well-defined RV tissue configuration and organization (Fig. 4*A*), whereas that of rats from the SH group presented signs of tissue disorganization, excessive extracellular matrix (black arrow), and inflammatory infiltrate (red arrow) in some regions. The presence of type I collagen was observed in the RV of rats from the SH group (white arrow) (Fig. 4*B*). Animals in the SH group had lower percentage of cardiomyocytes (Fig. 4*C*) and higher percentages of extracellular matrix (Fig. 4*D*), inflammatory infiltrate (Fig. 4*E*), and type I collagen (Fig. 4*F*) compared with those in the SC and EH groups ($P < 0.05$).

Regarding oxidative stress in the RV, no between-group differences were found in the activity of CAT (Fig. 5*A*), SOD (Fig. 5*B*), and GST (Fig. 5*C*), and in the levels of MDA (Fig. 5*D*). Nevertheless, rats in the SH group showed a reduction ($P < 0.05$) in NO activity (Fig. 5*E*) and an increase in PC compared with those in the SC and EH groups (Fig. 5*F*). In addition, it was observed that animals in the EH group showed an increase ($P < 0.05$) in PC activity compared with animals in the SC group.

### Pulmonary Remodeling and Oxidative Stress

The representative photomicrographs of the right lung (Fig. 6*A*) show that rats in the SH group exhibited lung microarchitecture [e.g., alveolar septum (white arrow); and alveoli (black arrow)] visibly distinct from those of animals in the SC and EH groups. The rats from the SH group had a higher ($P < 0.05$) percentage of alveolar septum (Fig. 6*B*); and a lower ($P < 0.05$) percentage of pulmonary alveoli than those in the SC and EH groups (Fig. 6*C*).

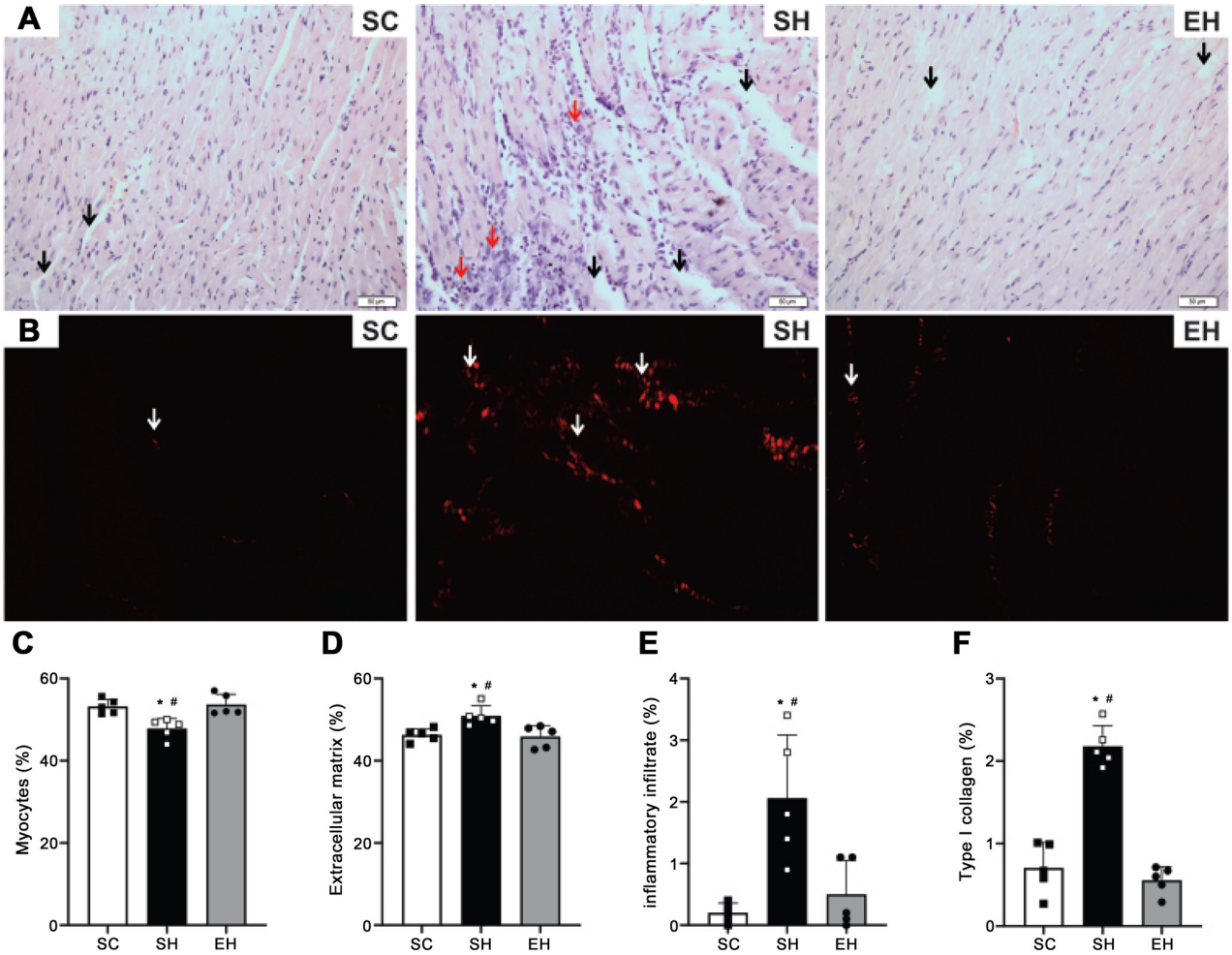


**Figure 4.** Effects of combined physical training on the right ventricle. *A*: representative photomicrographs of tissue stained with H&E. Scale bar = 50 μm. *B*: representative photomicrographs of tissue stained with picrosirius red. Scale bar = 50 μm. *C*: percentage of cardiomyocytes. *D*: percentage of extracellular matrix. *E*: percentage of inflammatory infiltrate. *F*: percentage of type I collagen. Data are means ± SD of five rats in each group. EH, exercise hypertensive; H&E, hematoxylin-eosin; SC, sedentary control; SH, sedentary hypertensive. One-way ANOVA followed by Tukey's post hoc test. *$P < 0.05$ vs. SC; #$P < 0.05$ vs. EH.

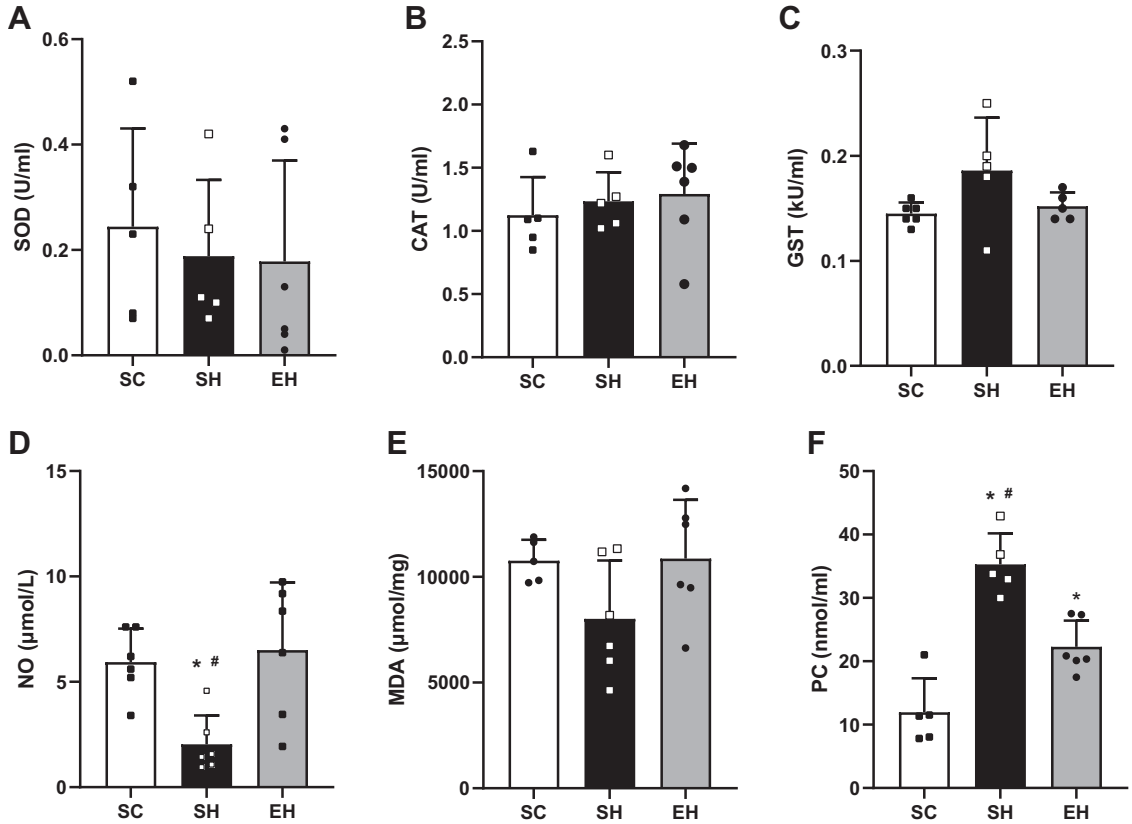


**Figure 5.** Effects of combined physical training on right ventricular oxidative stress biomarkers. Superoxide dismutase (SOD; *A*), catalase (CAT; *B*), glutathione S-transferase (GST; *C*), nitric oxide (NO; *D*), malondialdehyde (MDA; *E*), and protein carbonyl (PC; *F*). Data are means ± SD of five and six rats in each group. EH, exercise hypertensive; SC, sedentary control; SH, sedentary hypertensive. One-way ANOVA followed by Tukey's post hoc test. *$P <$ 0.05 vs. SC; #$P <$ 0.05 vs. EH.

Concerning the lung oxidative stress, the rats in the SH group exhibited a decrease ($P < 0.05$) in the activity of CAT (Fig. 7*A*), GST (Fig. 7*C*), and NO concentration (Fig. 7*E*) compared with those in the SC and EH groups. No between-group differences were observed for the activity of SOD (Fig. 7*B*) and the levels of MDA (Fig. 7*D*) and PC (Fig. 7*F*).

## DISCUSSION

We investigated whether combined physical exercise training of moderate intensity executed during the development of MCT-induced PAH hinders the progression of pulmonary and right heart harmful functional and structural

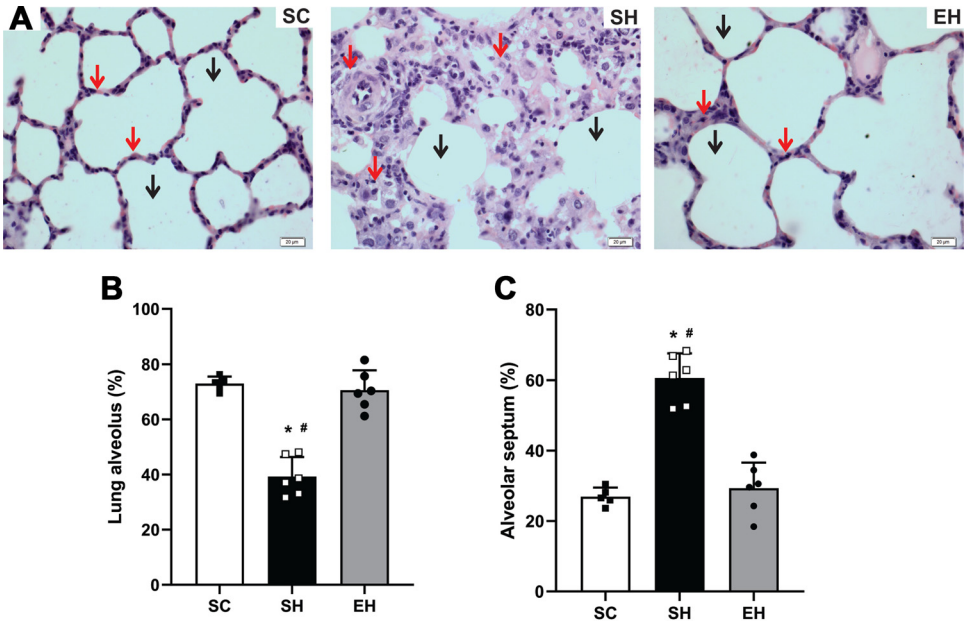


**Figure 6.** Histomorphometry of the right lung. *A*: representative photomicrograph of the right lung (hematoxylin-eosin, in cross section). *B*: percentage of pulmonary alveoli among the tissue elements of the lung. *C*: percentage of pulmonary alveoli among the tissue elements of the lung. Data are means ± SD of 10 images per animal in each group (5 to 6 animals per group). EH, hypertensive exercise; SC, sedentary control; SH, hypertensive sedentary. One-way ANOVA followed by Tukey's post hoc test. *$P <$ 0.05 vs. SC; #$P <$ 0.05 vs. EH.

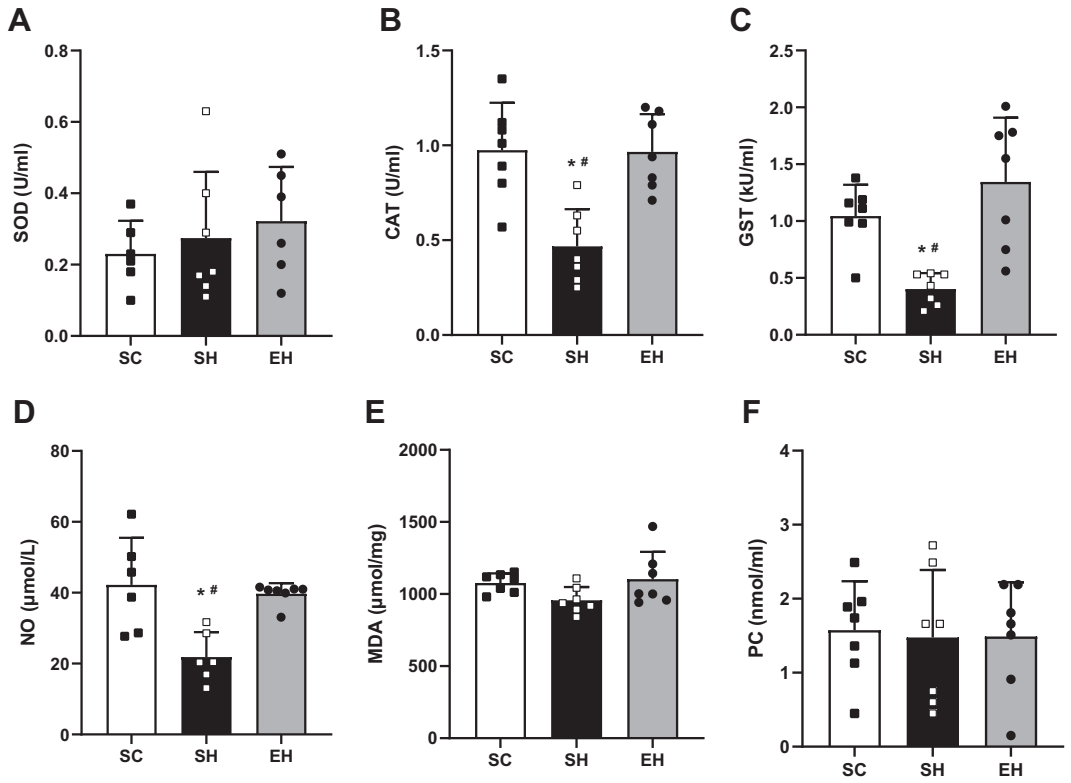


**Figure 7.** Effects of combined physical training on lung oxidative stress biomarkers. Superoxide dismutase (SOD; *A*), catalase (CAT; *B*), glutathione S-transferase (GST; *C*), nitric oxide (NO; *D*), malondialdehyde (MDA; *E*), and protein carbonyl (PC; *F*). Data are means ± SD of six and seven rats in each group. EH, exercise hypertensive; SC, sedentary control; SH, sedentary hypertensive. One-way ANOVA followed by Tukey's post hoc test. $*P < 0.05$ vs. SC; $\#P < 0.05$ vs. EH.

remodeling in rats. The hemodynamic findings revealed that the implemented physical exercise regimen preserved pulmonary artery resistance (i.e., TA/TE ratio) and right heart function (i.e., TAPSE), which were negatively affected by the MCT injection. These data align with prior results reported by our group, where both aerobic (29, 30) and resistance exercise training (17, 47) performed independently showed such beneficial effects. The mitigation of increases in pulmonary artery resistance might be attributed to the adequate bioavailability of NO, a potent vasodilator whose synthesis is stimulated by physical exercise (48). Indeed, in the present study, the levels of NO were conserved in the lung and RV tissues of exercised rats. Moreover, it is noteworthy that MCT induces oxidative stress in the cardiopulmonary vasculature resulting in endothelial damages and thus augmented pulmonary artery resistance (6). Despite not measuring oxidative stress biomarkers in the pulmonary artery, we observed changes in RV (i.e., increased CP and reduced NO) and lung (i.e., reduced CAT, GST, and NO) tissues of non-exercised rats from the SH group. More important, combined exercise avoided these negative alterations in rats from the EH group, which may help to explain the preservation of the pulmonary artery resistance in these animals.

Regarding the maintenance of right heart function in response to combined exercise observed in rats from the EH group, it is conceivable that the reduction in their pulmonary artery resistance has influenced such an advantage since it alleviates the RV pressure and hence adverse remodeling (17). To illustrate, our data show that these animals were protected against RV tissue harmful structural remodeling (i.e., reduction in the percentage of cardiomyocytes and increases in the percentages of extracellular matrix, inflammatory infiltrate, and total collagen), thus displaying normal right heart functionality. Moreover, some structural benefits caused by combined exercise were found in the lung tissue of these animals like no increases in the percentages of alveolar septum and alveoli. Although the exact mechanisms underlying such effects are not fully elucidated, it is possible that exercise has sustained the $H_2O_2$/VEGF/p-Akt signaling for pulmonary angiogenesis (49). Previous studies have demonstrated that pulmonary angiogenesis is crucial to adapt the pulmonary vascular system to stressful conditions such as PAH (50, 51). In addition, we noted that combined exercise preserved the activity of antioxidant enzymes (e.g., CAT and GST), and the production of NO in the lungs of rats with PAH. These biomarkers are vital components of the body's antioxidant defense system to neutralize reactive oxygen species and shield cells from oxidative damages (52). Furthermore, our combined exercise program retained the augment of oxidative stress in the RV of exercised rats by reducing CP and increasing NO levels. These results line up with the documented benefits of exercise in reducing oxidative stress (17, 53, 54). NO is well known for its antioxidant and anti-inflammatory properties playing a pivotal role in safeguarding the heart against myocardial remodeling (55). Therefore, both structural and biochemical benefits caused by combined exercise help to explain the preserved right heart function in the exercised hypertensive rats.

Along with the beneficial changes found in the RV tissue, at the cellular level, combined exercise kept the contractile function of isolated RV myocytes, which was impaired by MCT-induced PAH. Although cardiomyocytes from SH rats exhibited reduced amplitude and velocities of contraction and relaxation, as well as decreased amplitude and velocities to peak and to decay of the intracellular $Ca^{2+}$ transient than those from SC rats, such harms were not observed in cardiomyocytes from exercised rats. These exercise effects may be linked to some protection to the cellular $Ca^{2+}$ regulatory proteins. For example, sarcoplasmic reticulum $Ca^{2+}$ ATPase type 2a (SERCA2a) and ryanodine receptor 2 (RyR2) are the main responsible for removing $Ca^{2+}$ from the cytosol and thus regulate the relaxation velocities in cardiomyocytes (56). Although not analyzed in the present study, previous investigations reveal that moderate-intensity aerobic exercise increases the expression of SERCA2a and RyR2 in the RV of rats with MCT-induced PAH (57, 58) which leads to improved intracellular $Ca^{2+}$ relaxation's velocity.

Altogether, these functional, biochemical, and structural benefits promoted by the applied combined exercise seem to have resulted in improvements in the tolerance to physical exertion of the exercised rats. In fact, we observed a decline in the physical exertion of rats from the SH group, whereas those undergoing combined exercise exhibited enhanced tolerance to physical effort. Such increase may also be assisted by some beneficial effects of the combined exercise regime on skeletal muscle tissue, which helps avoiding muscle waste and dysfunction (17).

Finally, controlling the rat's climbing speed in the resistance training protocol was not feasible, and therefore, the precise regulation of the exercise intensity was limited. Nevertheless, despite such conditions, this study is groundbreaking in demonstrating that combined exercise training of moderate intensity executed during the development of MCT-induced PAH confers significant benefits to the pulmonary and right heart function and structure in rats.

### Conclusions

In conclusion, the applied combined exercise regime hinders the progression of pulmonary and right heart functional and structural harmful remodeling in rats with MCT-induced PAH. An attenuated progression of the disease impacts positively on its prognosis.

## DECLARATIONS

Ethics approval: The study protocol was approved by the Ethics Committee on Animal Use of the Federal University of Viçosa (CEUA-UFV; Protocol No. 02/2021).

## DATA AVAILABILITY

The datasets used and/or analyzed during the current study are available from the corresponding author upon reasonable request.

## ACKNOWLEDGMENTS

L. B. Leite is thankful to Coordenação de Aperfeiçoamento de Pessoal de Nível Superior—Brazil (CAPES) for the scholarship. A. J. Natali and M. Machado-Neves are thankful to CNPq—Brazil for the fellowships.

## GRANTS

This work was supported by the Fundação de Amparo à Pesquisa do Estado de Minas Gerais—Brasil (FAPEMIG)—Grant No. APQ-01485-22, Conselho Nacional de Desenvolvimento Científico e Tecnologico—Brasil (CNPq)—Grant No. 306956/2021-7, and Coordenação de Aperfeiçoamento de Pessoal de Nível Superior - Brasil (CAPES) – Finance Code 001.

## DISCLAIMERS

The supporters did not involve in the study design; data collection, analysis, and interpretation; the writing of the manuscript; and the decision to submit the manuscript for publication.

## DISCLOSURES

No conflicts of interest, financial or otherwise, are declared by the authors.

## AUTHOR CONTRIBUTIONS

L.B.L., L.L.S., B.A.F.d.S., T.R.D., M.A.C.-J., P.F., and A.J.N. conceived and designed research; L.B.L., L.L.S., A.M.O.P., B.A.F.d.S., T.R.D., M.Q.A., L.O.G.-E., M.A.C.-J., P.F., E.C.C.R., and A.J.N. performed experiments; L.B.L., L.L.S., A.M.O.P., B.A.F.d.S., T.R.D., T.I.S., M.Q.A., L.O.G.-E., M.A.C.-J., P.F., E.C.C.R., and A.J.N. analyzed data; L.B.L., A.M.O.P., T.I.S., M.Q.A., L.O.G.-E., M.A.C.-J., M.M.-N., E.C.C.R., and A.J.N. interpreted results of experiments; L.B.L., T.I.S., M.M.-N., E.C.C.R., and A.J.N. prepared figures; L.B.L., P.F., M.M.-N., and A.J.N. drafted manuscript; L.B.L. and A.J.N. edited and revised manuscript; L.B.L. and A.J.N. approved final version of manuscript.

## REFERENCES

1. **Kasahara Y**, **Kiyatake K**, **Tatsumi K**, **Sugito K**, **Kakusaka I**, **Yamagata S**, **Ohmori S**, **Kitada M**, **Kuriyama T.** Bioactivation of monocrotaline by P-450 3A in rat liver. *J Cardiovasc Pharmacol* 30: 124–129, 1997. doi:10.1097/00005344-199707000-00018.
2. **Meyrick B**, **Gamble W**, **Reid L.** Development of Crotalaria pulmonary hypertension: hemodynamic and structural study. *Am J Physiol Heart Circ Physiol* 239: H692–H702, 1980. doi:10.1152/ajpheart.1980.239.5.H692.
3. **Doggrell SA**, **Brown L.** Rat models of hypertension, cardiac hypertrophy and failure. *Cardiovasc Res* 39: 89–105, 1998. doi:10.1016/S0008-6363(98)00076-5.
4. **Garcia AR**, **Blanco I**, **Ramon L**, **Pérez-Sagredo J**, **Guerra-Ramos FJ**, **Martín-Ontiyuelo C**, **Tura-Ceide O**, **Pastor-Pérez F**, **Escribano-Subías P**, **Barberà JÁ.** Predictors of the response to phosphodiesterase-5 inhibitors in pulmonary arterial hypertension: an analysis of the Spanish registry. *Respir Res* 24: 223, 2023. doi:10.1186/s12931-023-02531-1.
5. **Aggarwal S**, **Gross CM**, **Sharma S**, **Fineman JR**, **Black SM.** Reactive oxygen species in pulmonary vascular remodeling. *Compr Physiol* 3: 1011–1034, 2013. doi:10.1002/cphy.c120024.
6. **DeMarco VG**, **Whaley-Connell AT**, **Sowers JR**, **Habibi J**, **Dellsperger KC.** Contribution of oxidative stress to pulmonary arterial hypertension. *World J Cardiol* 2: 316–324, 2010. doi:10.4330/wjc.v2.i10.316.
7. **Turck P**, **Fraga S**, **Salvador I**, **Campos-Carraro C**, **Lacerda D**, **Bahr A**, **Ortiz V**, **Hickmann A**, **Koetz M**, **Bello-Klein A**, **Henriques A**, **Agostini F**, **Araujo ASD.** Blueberry extract decreases oxidative stress and improves functional parameters in lungs from rats with pulmonary arterial hypertension. *Nutrition* 70: 110579, 2020. doi:10.1016/j.nut.2019.110579.
8. **Dianat M**, **Radan M**, **Mard SA**, **Sohrabi F**, **Saryazdi SSN.** Contribution of reactive oxygen species via the OXR1 signaling pathway in the pathogenesis of monocrotaline-induced pulmonary

arterial hypertension: the protective role of Crocin. *Life Sci* 256: 117848, 2020. doi:10.1016/j.lfs.2020.117848.

9. **Redout EM**, **Wagner MJ**, **Zuidwijk MJ**, **Boer C**, **Musters RJ**, **van Hardeveld C**, **Paulus WJ**, **Simonides WS.** Right-ventricular failure is associated with increased mitochondrial complex II activity and production of reactive oxygen species. *Cardiovasc Res* 75: 770–781, 2007. doi:10.1016/j.cardiores.2007.05.012.
10. **Farahmand F**, **Hill MF**, **Singal PK.** Antioxidant and oxidative stress changes in experimental cor pulmonale. *Mol Cell Biochem* 260: 21–29, 2004. doi:10.1023/b.0000026047.48534.50.
11. **Souza-Rabbo MP**, **Silva LF**, **Auzani JA**, **Picoral M**, **Khaper N**, **Belló-Klein A.** Effects of a chronic exercise training protocol on oxidative stress and right ventricular hypertrophy in monocrotaline-treated rats. *Clin Exp Pharmacol Physiol* 35: 944–948, 2008. doi:10.1111/j.1440-1681.2008.04936.x.
12. **Türck P**, **Salvador IS**, **Campos-Carraro C**, **Ortiz V**, **Bahr A**, **Andrades M**, **Belló-Klein A**, **Araujo AS.** Blueberry extract improves redox balance and functional parameters in the right ventricle from rats with pulmonary arterial hypertension. *Eur J Nutr* 61: 373–386, 2022. doi:10.1007/s00394-021-02642-9.
13. **Colombo R**, **Siqueira R**, **Conzatti A**, **de Lima Seolin BG**, **Fernandes TRG**, **Godoy AEG**, **Litvin IE**, **Silva JM**, **Tucci PJ**, **da Rosa Araújo AS**, **Belló-Klein A.** Exercise training contributes to $H_2O_2$/VEGF signaling in the lung of rats with monocrotaline-induced pulmonary hypertension. *Vascul Pharmacol* 87: 49–59, 2016. doi:10.1016/j.vph.2016.06.006.
14. **Horiguchi M**, **Kojima H**, **Sakai H**, **Kubo H**, **Yamashita C.** Pulmonary administration of integrin-nanoparticles regenerates collapsed alveoli. *J Control Release* 187: 167–174, 2014. doi:10.1016/j.jconrel.2014.05.050.
15. **Nogueira-Ferreira R**, **Moreira-Gonçalves D**, **Silva AF**, **Duarte JA**, **Leite-Moreira A**, **Ferreira R**, **Henriques-Coelho T.** Exercise preconditioning prevents MCT-induced right ventricle remodeling through the regulation of TNF superfamily cytokines. *Int J Cardiol* 203: 858–866, 2016. doi:10.1016/j.ijcard.2015.11.066.
16. **Suzuki T**, **Sato Y**, **Yamamoto H**, **Kato T**, **Kitase Y**, **Ueda K**, **Mimatsu H**, **Sugiyama Y**, **Onoda A**, **Saito S**, **Takahashi Y**, **Nakayama T**, **Hayakawa M.** Mesenchymal stem/stromal cells stably transduced with an inhibitor of CC chemokine ligand 2 ameliorate bronchopulmonary dysplasia and pulmonary hypertension. *Cytotherapy* 22: 180–192, 2020. doi:10.1016/j.jcyt.2020.01.009.
17. **Soares LL**, **Leite LB**, **Ervilha LOG**, **Pelozin BRA**, **Pereira NP**, **da Silva BAF**, **Portes AMO**, **Drummond FR**, **de Rezende LMT**, **Fernandes T**, **Oliveira EM**, **Neves MM**, **Reis ECC**, **Natali AJ.** Resistance exercise training benefits pulmonary, cardiac, and muscular structure and function in rats with stable pulmonary artery hypertension. *Life Sci* 332: 122128, 2023. doi:10.1016/j.lfs.2023.122128.
18. **Corssac GB**, **Bonetto JP**, **Campos-Carraro C**, **Cechinel LR**, **Zimmer A**, **Parmeggiani B**, **Grings M**, **Carregal VM**, **Massensini AR**, **Siqueira I**, **Leipnitz G**, **Belló-Klein A.** Pulmonary arterial hypertension induces the release of circulating extracellular vesicles with oxidative content and alters redox and mitochondrial homeostasis in the brain of rats. *Hypertens Res* 44: 918–931, 2021. doi:10.1038/s41440-021-00660-y.
19. **Mikhael M**, **Makar C**, **Wissa A**, **Le T**, **Eghbali M**, **Umar S.** Oxidative stress and its implications in the right ventricular remodeling secondary to pulmonary hypertension. *Front Physiol* 10: 1233, 2019. doi:10.3389/fphys.2019.01233.
20. **Puukila S**, **Fernandes RO**, **Türck P**, **Carraro CC**, **Bonetto JHP**, **de Lima-Seolin BG**, **da Rosa Araujo AS**, **Belló-Klein A**, **Boreham D**, **Khaper N.** Secoisolariciresinol diglucoside attenuates cardiac hypertrophy and oxidative stress in monocrotaline-induced right heart dysfunction. *Mol Cell Biochem* 432: 33–39, 2017. doi:10.1007/s11010-017-2995-z.
21. **Takimoto E**, **Kass DA.** Role of oxidative stress in cardiac hypertrophy and remodeling. *Hypertension* 49: 241–248, 2007. doi:10.1161/01.HYP.0000254415.31362.a7.
22. **Giordano FJ.** Oxygen, oxidative stress, hypoxia, and heart failure. *J Clin Invest* 115: 500–508, 2005. doi:10.1172/JCI24408.
23. **Zima AV**, **Blatter LA.** Redox regulation of cardiac calcium channels and transporters. *Cardiovasc Res* 71: 310–321, 2006. doi:10.1016/j.cardiores.2006.02.019.
24. **Whelton PK**, **Carey RM**, **Aronow WS**, **Casey DE**, **Collins KJ**, **Dennison Himmelfarb C**, **DePalma SM**, **Gidding S**, **Jamerson KA**, **Jones DW**, **MacLaughlin EJ**, **Muntner P**, **Ovbiagele B**, **Smith SC**, **Spencer CC**, **Stafford RS**, **Taler SJ**, **Thomas RJ**, **Williams KA**, **Williamson JD**, **Wright JT.** ACC/AHA/AAPA/ABC/ACPM/AGS/APhA/ASH/ASPC/NMA/PCNA guideline for the prevention, detection, evaluation, and management of high blood pressure in adults: a report of the American College of Cardiology/American Heart Association Task Force on clinical practice guidelines. *Hypertension* 71: e13–e115, 2018. doi:10.1161/HYP.0000000000000065.
25. **Unger T**, **Borghi C**, **Charchar F**, **Khan NA**, **Poulter NR**, **Prabhakaran D**, **Ramirez A**, **Schlaich M**, **Stergiou GS**, **Tomaszewski M**, **Wainford RD**, **Williams B**, **Schutte AE.** 2020 International Society of Hypertension Global Hypertension Practice Guidelines. *Hypertension* 75: 1334–1357, 2020. doi:10.1161/HYPERTENSIONAHA.120.15026.
26. **González-Saiz L**, **Fiuza-Luces C**, **Sanchis-Gomar F**, **Santos-Lozano A**, **Quezada-Loaiza CA**, **Flox-Camacho A**, **Munguía-Izquierdo D**, **Ara I**, **Santalla A**, **Morán M**, **Sanz-Ayan P**, **Escribano-Subías P**, **Lucia A.** Benefits of skeletal-muscle exercise training in pulmonary arterial hypertension: the WHOLEi + 12 trial. *Int J Cardiol* 231: 277–283, 2017. doi:10.1016/j.ijcard.2016.12.026.
27. **Kabitz H-J**, **Bremer H-C**, **Schwoerer A**, **Sonntag F**, **Walterspacher S**, **Walker DJ**, **Ehlken N**, **Staehler G**, **Windisch W**, **Grünig E.** The combination of exercise and respiratory training improves respiratory muscle function in pulmonary hypertension. *Lung* 192: 321–328, 2014. doi:10.1007/s00408-013-9542-9.
28. **Mainguy V**, **Maltais F**, **Saey D**, **Gagnon P**, **Martel S**, **Simon M**, **Provencher S.** Peripheral muscle dysfunction in idiopathic pulmonary arterial hypertension. *Thorax* 65: 113–117, 2010. doi:10.1136/thx.2009.117168.
29. **Silva F**, **Drummond R**, **Fidelis MR**, **Freitas MO**, **Leal TF**, **Teixeira LM**, **de Rezende A**, **de Moura G**, **Reis ECC**, **Natali AJ.** Continuous aerobic exercise prevents detrimental remodeling and right heart myocyte contraction and calcium cycling dysfunction in pulmonary artery hypertension. *J Cardiovasc Pharmacol* 77: 69–78, 2021. doi:10.1097/FJC.0000000000000928.
30. **Soares LL**, **Drummond FR**, **Rezende LMT**, **Lopes Dantas Costa AJ**, **Leal TF**, **Fidelis MR**, **Neves MM**, **Prímola-Gomes TN**, **Carneiro-Junior MA**, **Carlo Reis EC**, **Natali AJ.** Voluntary running counteracts right ventricular adverse remodeling and myocyte contraction impairment in pulmonary arterial hypertension model. *Life Sci* 238: 116974, 2019. doi:10.1016/j.lfs.2019.116974.
31. **Natali AJ**, **Fowler ED**, **Calaghan SC**, **White E.** Voluntary exercise delays heart failure onset in rats with pulmonary artery hypertension. *Am J Physiol Heart Circ Physiol* 309: H421–H424, 2015. doi:10.1152/ajpheart.00262.2015.
32. **Zimmer A**, **Teixeira RB**, **Bonetto JHP**, **Siqueira R**, **Carraro CC**, **Donatti LM**, **Hickmann A**, **Litvin IE**, **Godoy AEG**, **Araujo AS**, **Colombo R**, **Belló-Klein A.** Effects of aerobic exercise training on metabolism of nitric oxide and endothelin-1 in lung parenchyma of rats with pulmonary arterial hypertension. *Mol Cell Biochem* 429: 73–89, 2017. doi:10.1007/s11010-016-2937-1.
33. **Hornberger TA Jr**, **Farrar RP.** Physiological hypertrophy of the FHL muscle following 8 weeks of progressive resistance exercise in the rat. *Can J Appl Physiol* 29: 16–31, 2004. doi:10.1139/h04-002.
34. **Sanches IC**, **Conti FF**, **Sartori M**, **Irigoyen MC**, **De Angelis K.** Standardization of resistance exercise training: effects in diabetic ovariectomized rats. *Int J Sports Med* 35: 323–329, 2014. doi:10.1055/s-0033-1351254.
35. **Sahn DJ**, **DeMaria A**, **Kisslo J**, **Weyman A.** Recommendations regarding quantitation in M-mode echocardiography: results of a survey of echocardiographic measurements. *Circulation* 58: 1072–1083, 1978. doi:10.1161/01.CIR.58.6.1072.
36. **Leite LB**, **Soares LL**, **Portes AMO**, **Soares TI**, **da Silva BAF**, **Dias TR**, **Costa SFF**, **Guimarães-Ervilha LO**, **Assis MQ**, **Lavorato VN**, **da Silva AN**, **Machado-Neves M**, **Reis ECC**, **Natali AJ.** Combined physical training protects the left ventricle from structural and functional damages in experimental pulmonary arterial hypertension. *Clin Hypertens* 30: 12, 2024. doi:10.1186/s40885-024-00270-z.
37. **Carneiro-Júnior MA**, **Quintão-Júnior JF**, **Drummond LR**, **Lavorato VN**, **Drummond FR**, **da Cunha DNQ**, **Amadeu MA**, **Felix LB**, **de Oliveira EM**, **Cruz JS**, **Prímola-Gomes TN**, **Mill JG**, **Natali AJ.** The benefits of endurance training in cardiomyocyte function in hypertensive rats are reversed within four weeks of detraining. *J Mol Cell Cardiol* 57: 119–128, 2013. doi:10.1016/j.yjmcc.2013.01.013.
38. **Kondo RP**, **Dederko DA**, **Teutsch C**, **Chrast J**, **Catalucci D**, **Chien KR**, **Giles WR.** Comparison of contraction and calcium handling between right and left ventricular myocytes from adult mouse heart: a

role for repolarization waveform. *J Physiol* 571: 131–146, 2006 [Erratum in *J Physiol* 571: 499, 2006]. doi:10.1113/jphysiol.2005.101428.
39. **Wang Z**, **Patel JR**, **Schreier DA**, **Hacker TA**, **Moss RL**, **Chesler NC.** Organ-level right ventricular dysfunction with preserved Frank–Starling mechanism in a mouse model of pulmonary arterial hypertension. *J Appl Physiol (1985)* 124: 1244–1253, 2018. doi:10.1152/japplphysiol.00725.2017.
40. **Hadwan MH**, **Abed HN.** Data supporting the spectrophotometric method for the estimation of catalase activity. *Data Brief* 6: 194–199, 2016. doi:10.1016/j.dib.2015.12.012.
41. **Dieterich S**, **Bieligk U**, **Beulich K**, **Hasenfuss G**, **Prestle J.** Gene expression of antioxidative enzymes in the human heart: increased expression of catalase in the end-stage failing heart. *Circulation* 101: 33–39, 2000. doi:10.1161/01.CIR.101.1.33.
42. **Habig WH**, **Pabst MJ**, **Jakoby WB.** Glutathione S-transferases: the first enzymatic step in mercapturic acid formation. *J Biol Chem* 249: 7130–7139, 1974.
43. **Buege AJ**, **Aust DS.** Microsomal lipid peroxidation. *Methods Enzymol* 52: 302–310, 1978. doi:10.1016/S0076-6879(78)52032-6.
44. **Tsikas D.** Analysis of nitrite and nitrate in biological fluids by assays based on the Griess reaction: appraisal of the Griess reaction in the L-arginine/nitric oxide area of research. *J Chromatogr B Analyt Technol Biomed Life Sci* 851: 51–70, 2007. doi:10.1016/j.jchromb.2006.07.054.
45. **Levine RL**, **Williams JA**, **Stadtman ER**, **Shacter E.** Carbonyl assays for determination of oxidatively modified proteins. *Methods Enzymol* 233: 346–357, 1994. doi:10.1016/s0076-6879(94)33040-9.
46. **Lowry OH**, **Rosebrough NJ**, **Farr AL**, **Randall RJ.** Protein measurement with the Folin phenol reagent. *J Biol Chem* 193: 265–275, 1951. doi:10.1016/S0021-9258(19)52451-6.
47. **Soares LL**, **Leite LB**, **Ervilha LOG**, **Silva BAFD**, **Freitas MO**, **Portes AMO**, **Rezende LMT**, **Drummond FR**, **Carneiro-Júnior MA**, **Neves MM**, **Reis ECC**, **Natali AJ.** Resistance exercise training mitigates left ventricular dysfunctions in pulmonary artery hypertension model. *Arq Bras Cardiol* 119: 574–584, 2022. doi:10.36660/abc.20210681.
48. **Ashor AW**, **Lara J**, **Siervo M**, **Celis-Morales C**, **Oggioni C**, **Jakovljevic DG**, **Mathers JC.** Exercise modalities and endothelial function: a systematic review and dose-response meta-analysis of randomized controlled trials. *Sports Med* 45: 279–296, 2015. doi:10.1007/s40279-014-0272-9.
49. **Colombo R**, **Siqueira R**, **Becker CU**, **Fernandes TG**, **Pires KM**, **Valença SS**, **Souza-Rabbo MP**, **Araujo AS**, **Belló-Klein A.** Effects of exercise on monocrotaline-induced changes in right heart function and pulmonary artery remodeling in rats. *Can J Physiol Pharmacol* 91: 38–44, 2013. doi:10.1139/cjpp-2012-0261.
50. **Miao H**, **Qiu F**, **Zhu L**, **Jiang B**, **Yuan Y**, **Huang B**, **Zhang Y.** Novel angiogenesis strategy to ameliorate pulmonary hypertension. *J Thorac Cardiovasc Surg* 161: e417–e434, 2021. doi:10.1016/j.jtcvs.2020.03.044.
51. **Voelkel NF**, **Tuder RM**, **Bridges J**, **Arend WP.** Interleukin-1 receptor antagonist treatment reduces pulmonary hypertension generated in rats by monocrotaline. *Am J Respir Cell Mol Biol* 11: 664–675, 1994. doi:10.1165/ajrcmb.11.6.7946395.
52. **Ighodaro OM**, **Akinloye O.** First line defence antioxidants—superoxide dismutase (SOD), catalase (CAT), and glutathione peroxidase (GPX): their fundamental role in the entire antioxidant defence grid. *Alex J Med* 54: 287–293, 2018. doi:10.1016/j.ajme.2017.09.001.
53. **Gimenes C**, **Gimenes R**, **Rosa CM**, **Xavier NP**, **Campos DH**, **Fernandes AA**, **Cezar MD**, **Guirado GN**, **Cicogna AC**, **Takamoto AH**, **Okoshi MP**, **Okoshi K.** Low intensity physical exercise attenuates cardiac remodeling and myocardial oxidative stress and dysfunction in diabetic rats. *J Diabetes Res* 2015: 457848, 2015. doi:10.1155/2015/457848.
54. **Andrade LHS**, **de Moraes WMAM**, **Matsuo Junior EH**, **de Orleans Carvalho de Moura E**, **Antunes HKM**, **Montemor J**, **Antonio EL**, **Bocalini DS**, **Serra AJ**, **Tucci PJE**, **Brum PC**, **Medeiros A.** Aerobic exercise training improves oxidative stress and ubiquitin proteasome system activity in heart of spontaneously hypertensive rats. *Mol Cell Biochem* 402: 193–202, 2015. doi:10.1007/s11010-015-2326-1.
55. **Xu X**, **Zhao W**, **Lao S**, **Wilson BS**, **Erikson JM**, **Zhang JQ.** Effects of exercise and L-arginine on ventricular remodeling and oxidative stress. *Med Sci Sports Exerc* 42: 346–354, 2010. doi:10.1249/MSS.0b013e3181b2e899.
56. **Bers DM.** Cardiac excitation-contraction coupling. *Nature* 415: 198–205, 2002. doi:10.1038/415198a.
57. **Moreira-Gonçalves D**, **Ferreira R**, **Fonseca H**, **Padrão AI**, **Moreno N**, **Silva AF**, **Vasques-Nóvoa F**, **Gonçalves N**, **Vieira S**, **Santos M**, **Amado F**, **Duarte JA**, **Leite-Moreira AF**, **Henriques-Coelho T.** Cardioprotective effects of early and late aerobic exercise training in experimental pulmonary arterial hypertension. *Basic Res Cardiol* 110: 57, 2015. doi:10.1007/s00395-015-0514-5.
58. **Pacagnelli FL**, **de Almeida Sabela AKD**, **Okoshi K**, **Mariano TB**, **Campos DHS**, **Carvalho RF**, **Cicogna AC**, **Vanderlei LCM.** Preventive aerobic training exerts a cardioprotective effect on rats treated with monocrotaline. *Int J Exp Pathol* 97: 238–247, 2016 [Erratum in *Int J Exp Pathol* 99: 145, 2018]. doi:10.1111/iep.12166.